Acta Oceanol. Sin., 2023, Vol. 42, No. 1, P. 103–108
https://doi.org/10.1007/s13131-022-2038-9
http://www.aosocean.com
E-mail: ocean2@hyxb.org.cn

Application of an optical nitrate profiler to high- and low-turbidity coastal shelf waters

Yanpei Zhuang[1, 2], Yangjie Li[2], Xizhen Liu[3], Shichao Tian[4], Bin Wang[2], Zhongqiang Ji[2], Haiyan Jin[2, 5*], Jianfang Chen[2, 5]

[1] Polar and Marine Research Institute, Jimei University, Xiamen 361000, China

[2] Key Laboratory of Marine Ecosystem Dynamics, Second Institute of Oceanography, Ministry of Natural Resources, Hangzhou 310012, China

[3] Marine Monitoring and Forecasting Center of Zhejiang Province, Hangzhou 310000, China

[4] Institute for Geology, University of Hamburg, Hamburg 20000, Germany

[5] State Key Laboratory of Satellite Ocean Environment Dynamics, Second Institute of Oceanography, Ministry of Natural Resources, Hangzhou 310012, China

Received 31 December 2021; accepted 7 February 2022

Abstract

Here, we report the results of high-resolution nitrate measurements using an optical nitrate profiler (*in situ* ultraviolet spectrophotometer, ISUS) along transect across a high-turbidity shelf (East China Sea) and a low-turbidity shelf (Chukchi Sea). The ISUS-measured nitrate concentrations closely reproduced the results measured by conventional bottle methods in low-turbidity waters. However, for high-turbidity waters of the East China Sea (salinity<30), a correction factor of 1.19 was required to match the standard bottle measurements. The high-resolution ISUS data revealed subtle spatial variability (e.g., a subsurface nitrate minimum) that may have been missed if based solely on bottle results. Four main structures of the nitracline on the East China Sea are apparent from the ISUS nitrate profile. High-resolution nitrate data are important for studying nitrate budgets and nutrient dynamics on continental shelves.

Key words: high-resolution nitrate measurements, *in situ* ultraviolet spectrophotometer (ISUS), nutrient dynamics, nitracline, East China Sea, Chukchi Sea

Citation: Zhuang Yanpei, Li Yangjie, Liu Xizhen, Tian Shichao, Wang Bin, Ji Zhongqiang, Jin Haiyan, Chen Jianfang. 2023. Application of an optical nitrate profiler to high- and low-turbidity coastal shelf waters. Acta Oceanologica Sinica, 42(1): 103–108, doi: 10.1007/s13131-022-2038-9

1 Introduction

Nitrate in the ocean is an essential nutrient for marine microorganisms and influences marine ecosystems and the carbon cycle via its role in regulating biological production (Bauer et al., 2013; Cloern, 2001; Wang et al., 2003; Zhai and Dai, 2009). Excess or insufficient nitrate reserves can be detrimental to healthy coastal-marine ecosystems. Excessive nitrate input can cause ecological disasters and lead to environmental pressure in coastal oceans (e.g., Baltic Sea, East China Sea) (Rönnberg and Bonsdorff, 2004; Wang et al., 2012, 2017; Zhang et al., 2007). Nitrate availability is a limiting factor on phytoplankton production in some coastal oceans (e.g., Chukchi Sea) that are less impacted by human activity (Zhuang et al., 2020). The marine nitrate cycle is dynamic and affected by biological utilization and biogeochemical processes (Chen et al., 2019; Li et al., 2021; Zhuang et al., 2021a). Accurate and detailed data on the distribution of nitrate are therefore essential to our understanding of nitrogen cycling and ecosystem dynamics. However, it is difficult to obtain high-resolution profiles of nitrate distribution by using conventional methods of sample collection and lab colorimetric analysis.

There is a growing interest in the development of technology that could yield nitrate distribution data at high temporal and spatial resolution (Finch et al., 1998; Prien, 2007). Optical nitrate sensors use ultraviolet absorption spectroscopy and a processing algorithm (Sakamoto et al., 2017) to generate continuous real-time, *in situ* data on the nitrate content of seawater without the use of chemical reagents (Johnson and Coletti, 2002; Meyer et al., 2018; Pidcock et al., 2010). The *in situ* ultraviolet spectrophotometer (ISUS) has a response of 1 Hz and accuracy of ±0.5 μmol/L (Johnson et al., 2006), and has been integrated with autonomous underwater vehicles (Johnson and Needoba, 2008), autonomous profiling floats (Johnson et al., 2013), and conductive-temperature-depth system (Kaplunenko et al., 2013), oceanographic moorings (Johnson, 2010).

The ISUS nitrate sensor has potential for long-term monitoring and has improved our understanding of nutrient supply in the oligotrophic North Pacific (Johnson et al., 2010), nitrate load from the Mississippi River (Pellerin et al., 2014), annual nitrate drawdown at the ice edge of the Southern Ocean (Johnson et al., 2017), nitrate flux to estimate the export production in the Arctic

Foundation item: The National Key Research and Development Program of China under contract No. 2019YFE0120900; the Natural Science Foundation of Zhejiang Province under contract No. Y19D060024; the National Natural Science Foundation of China under contract Nos U1709202 and 41806228; the Project of Long-term Observation and Research Plan in the Changjiang Estuary and Adjacent East China Sea (LORCE).
*Corresponding author, E-mail: jinhaiyan@sio.org.cn

Ocean (Randelhoff and Guthrie, 2016), and nitrate flux across the sediment-water interface (Johnson et al., 2011). The ISUS nitrate sensor is also capable of high-resolution mapping of nitrate concentrations from the polar ocean to eastern Pacific seawater (Sakamoto et al., 2009). However, the ISUS sensor is rarely used in high-turbidity waters and often ceases to function in such waters (Khandelwal et al., 2020).

In this paper, we describe the application of the ISUS nitrate sensor on two typical shelves: the high-turbidity East China Sea, which is influenced by the Changjiang River, and the low-turbidity Arctic marginal Chukchi Sea. We compare and discuss the capabilities of the ISUS nitrate profiler on the two shelves, to observe the detailed differences in nitrate distribution and nitracline structure between high- and low-turbidity shelves.

2 Materials and methods

2.1 *Study site*

Data were collected at 13 sites along 2 transects across the East China Sea during summer 2011 and at 9 sites across the Chukchi Sea during summer 2014 (Fig. 1, Tables S1 and S2). The East China Sea is a typical high-turbidity shelf with an excessive nitrate load from the Changjiang River (Yan et al., 2003). The shelf is generally strongly stratified, with the summer extension of the Changjiang River plume overlying the colder and saltier shelf water. The Chukchi Sea is a low-turbidity shelf with little human impact and relatively low nitrate content (Zhuang et al., 2020). The distribution of nutrients over the shelf is strongly influenced by the Pacific Ocean inflow (Zhuang et al., 2016).

2.2 *Data collection*

Seawater was filtered through acid-cleaned cellulose acetate membranes (0.45 μm) and stored at –20°C in a freezer. Nitrate plus nitrite concentration was measured with standard colorimetric methods using a continuous flow analyzer (Skalar San++, Breda, Netherlands) in a laboratory onshore (samples from the East China Sea; Key Laboratory of Marine Ecosystem and Biogeochemistry, Hangzhou, China) or onboard a research vessel (samples from the Chukchi Sea; the icebreaker *Xuelong*). Nitrite was measured using the spectrometric method onboard the research vessels. Nitrate and nitrite bottle samples were analyzed according to Grasshoff et al. (2009). Analytical accuracy was ±2% and the detection limit was 0.1 μmol/L.

High-resolution nitrate profiles were obtained using a conductive-temperature-depth system integrated with an ISUS (serial number 217, Satlantic; Halifax, Canada). Applicable water temperature and salinity of the ISUS ranges from –2℃ to 35℃ and from 0 to 35, respectively. Calibration parameters for temperature and salinity-dependent corrections are loaded onto the instrument and applied for the nitrate calculations. Before the sensor was deployed, the ISUS was warmed up for 10 min to stabilize the instrument. Instrument stability was checked with ultra-clean de-ionized water (DIW) once a day, to minimize the effects of long-term drift caused by changes in optical properties. The accuracy of the ISUS was ±0.5 μmol/L, which was obtained by measuring a range of 0–40 μmo/L nitrate.

3 Assessment and discussion

3.1 *Capability of ISUS on high- and low-turbidity shelves*

Figure 2 compares the nutrient data and vertical profiles obtained by ISUS for the high-turbidity shelf (East China Sea) and low-turbidity shelf (Chukchi Sea). The East China Sea is one of the most turbid shelves in the world, receiving an average of

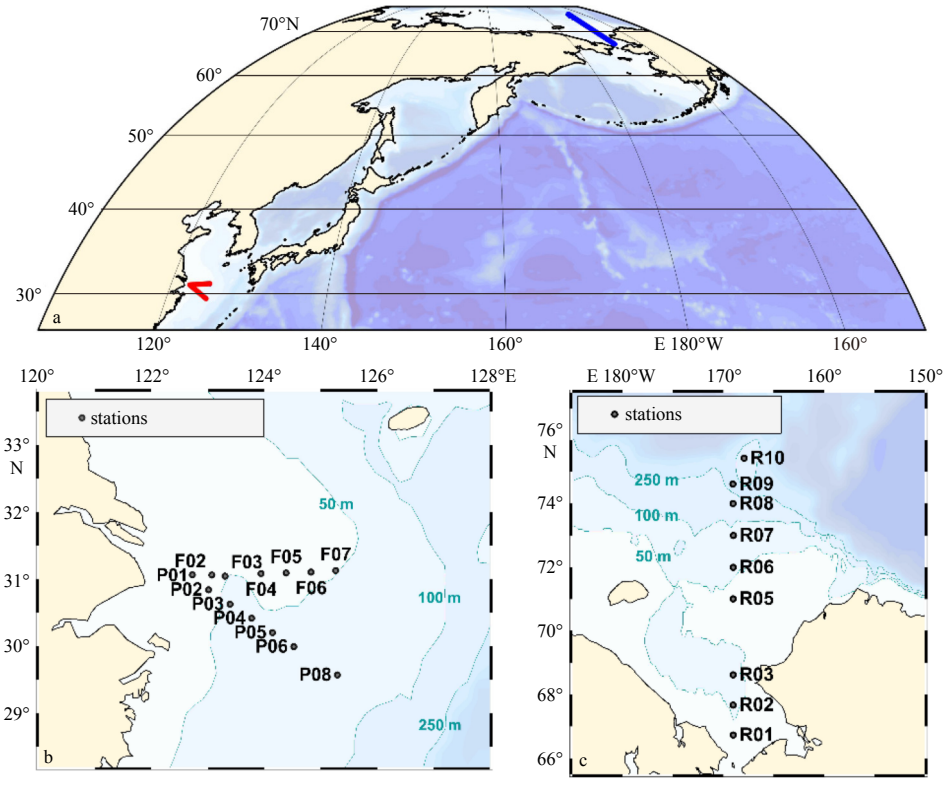

Fig. 1. Sampling sites on the East China Sea (red line in a and black dots in b) during summer 2011 and those on the Chukchi Sea (blue line in a and black dots in c) during summer 2014. The 50 m, 100 m, and 250 m isobaths are shown.

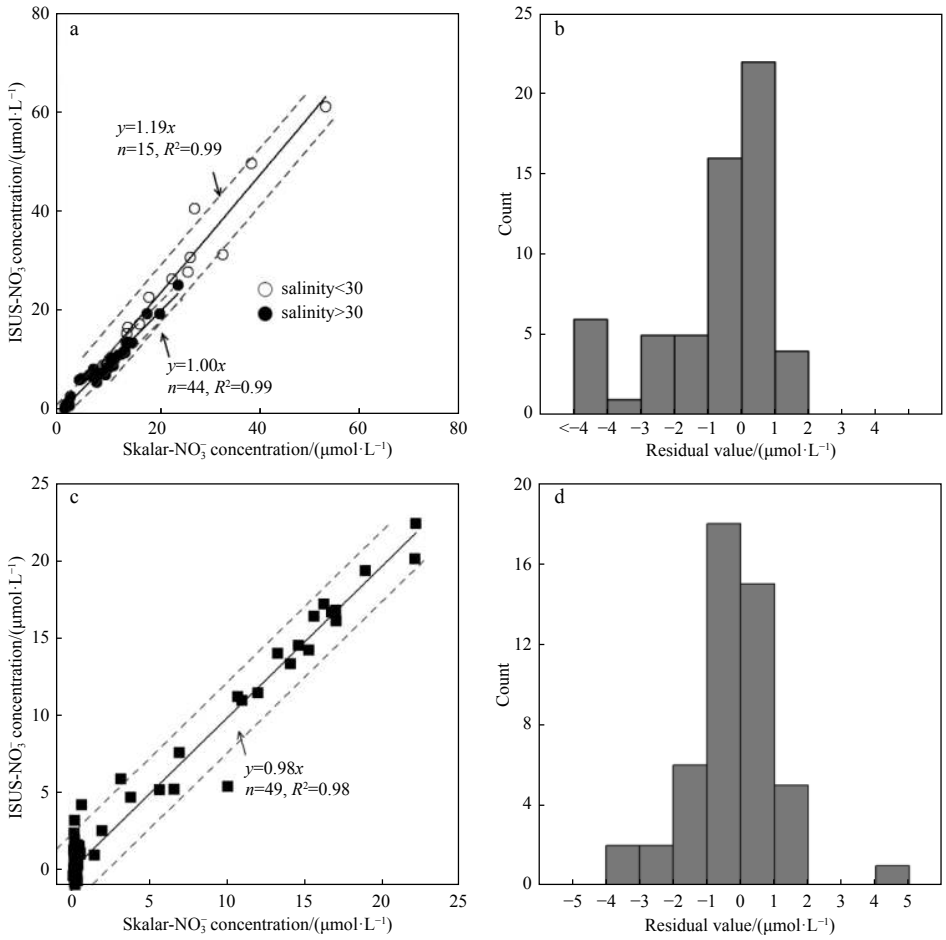

Fig. 2. Capability of *in situ* ultraviolet spectrophotometer (ISUS) on a high-turbidity shelf (East China Sea) and a low-turbidity shelf (Chukchi Sea). Relationship between the two datasets (a) and histogram of the residual (b) between ISUS-NO_3^- and Skalar-NO_3^- on the East China Sea during summer 2011. The c and d demonstrate similar relationship with a and b, but for the Chukchi Sea during summer 2014. The solid and dashed lines in a and c are linear regression lines and one standard deviation, respectively.

2.4×10^8 t/a of terrestrial material via the Changjiang River (Liu et al., 2007). The Changjiang River diluted water, defined as salinity<30 (Chen and Wang, 1999), contains extremely high contents of suspended particulate matter (SPM) that exceed 5 000 g/m^3 (Mao et al., 2012) and nitrate concentrations that exceed 120 μmol/L (Liu et al., 2016) in some regions. On the East China Sea transects, SPM was found at contents of 8.2–89.6 g/m^3 with an average of (27.8±15.5) g/m^3, and the highest concentration in the coastal water (Table S1). In contrast, the average SPM concentration on the Chukchi shelf was (3.6±1.1) g/m^3 (Table S2).

As shown in Fig. 2a, the ISUS-measured nitrate (ISUS-NO_3^-) is consistent with the Skalar-measured results (Skalar-NO_3^-) (y=1.00x) with a standard deviation of ±1 μmol/L for 44 pairs of data in the shelf water with salinity>30 in the East China Sea. In the shelf water with salinity<30, ISUS-NO_3^- data are higher than Skalar-NO_3^- data (y=1.19x), with a standard deviation of ±4.3 μmol/L (Fig. 2a). A correction of linear deviation on the high side by a factor of 1.19 was required in high-turbidity water (salinity< 30) of the East China Sea. The residual between the Skalar-NO_3^- and ISUS-NO_3^- data shows a normal distribution, except when the residual value is lower than –4 μmol/L, which reflects the deviation of the two methods when applied to shelf water with salinity<30 (Fig. 2b). In contrast, ISUS-NO_3^- and Skalar-NO_3^- measurements in the low-turbidity Chukchi Sea are in good agreement (y=0.98x), with a standard deviation of ±1.3 μmol/L (Fig. 2c); residual values show a normal distribution (Fig. 2d).

The results show that ISUS-NO_3^- data are consistent with Skalar-NO_3^- data in low-turbidity water, whereas a correction needs to be applied in high-turbidity water. Since chromophoric dissolved organic matter (CDOM) has a spectral component to its absorption curve, it may have a greater effect on the final nitrate calculation made using ISUS (MacIntyre et al., 2009). The estimated CDOM export flux from the Changjiang River at up to 2.04×10^{12} m^2/a (Guo et al., 2014), and CDOM in the estuarine turbidity maximum zones of the East China Sea is conservative (Guo et al., 2007). We therefore speculate that the high concentrations of CDOM associated with large amounts of suspended particulate matter caused the nitrate overestimation by the ISUS in the high-turbidity water. Nitrite exhibits similar characteristics with nitrate in the absorption band and has an interference on ISUS-NO_3^- measurement, however, nitrite concentrations are generally <1 μmol/L in the marine environment (Johnson and Coletti, 2002). In summary, the performance of the ISUS instrument in low-turbidity water is encouraging, and the limitations in high-turbidity waters can be addressed by applying a correction.

3.2 *High-resolution measurements to quantify spatial variability in nitrate contents*

In this study, high-resolution ISUS measurements and conventional techniques (discrete water bottle sampling) yield con-

sistent patterns of nitrate distribution across the East China Sea and Chukchi Sea (Fig. 3). The nitrate concentration shows a gradual decrease in the upper water column (<20 m) across the East China Sea, and two high-concentration patches in the Chukchi Sea (Fig. 3). Despite their different sampling frequencies, both methods identified the main nitrate trends as assessed using the spatial visualization software Ocean Data View version 4.4.1 (Schlitzer, 2018). The conventional method was able to present the spatial variability of nitrate, especially on the Chukchi Sea where nutrients are less dynamic.

Conventional techniques can identify the general patterns of nitrate distribution, although their low sampling frequency means that they may fail to detect small-scale, sensitive changes, especially on dynamic shelves. The high-resolution cross-shelf nitrate data on the East China Sea show several important features. First, the ISUS-NO_3^- results show a subsurface nitrate minimum between 123.5°E and 125°E at~15 m depth (Fig. 3a), which may be attributed to an intrusion of low-nitrate water from the outer shelf. Based solely on the discrete samples, it is difficult to identify this subsurface nitrate minimum or to constrain its detailed extent. In addition, the ISUS-NO_3^- measurements reveal a near-bottom (35 m) low-nitrate concentration water mass in the middle of the shelf (near 124°E). If this water mass had been sampled using conventional techniques, it might have been evaluated as an erroneous result or missed entirely, since there was only one bottle collection in the water column (Fig. 3b). Most importantly, high-resolution measurements can detect subtle spatial variations in nitrate contents that are easily overlooked when using conventional techniques. The accurate monitoring of such detailed changes can provide important information on marine biogeochemical processes.

3.3 *High-resolution measurements enable observations of detailed changes in the nitracline*

Nitraclines commonly lead to aggregations of phytoplankton (Zhuang et al., 2021b), which are important for fisheries and outbreaks of harmful algae blooms. Given the importance of nitraclines in marine environmental monitoring and nutrient dynamics, the acquisition of high-resolution nitrate profiles is important in understanding nitracline changes and subsequent ecological responses. The detailed change of a nitracline is influenced not only by the interaction between different water masses (Zhou et al., 2015), but also by biological activity and remineralization (Chen et al., 2013). In the present study, high-resolution nitrate measurements by the ISUS provided a powerful method for evaluating the detailed structures of the nitracline, on both the high-turbidity East China Sea (Fig. S1) and the low-turbidity Chukchi Sea (Fig. S2).

The low-turbidity Chukchi Sea, which is less strongly influenced by riverine input, had a single nitracline. The nitracline was positively correlated with the halocline, and nitrate content increased with salinity (Fig. S2), which we ascribe to the input of low-nutrient meltwater (Zhuang et al., 2017). In contrast, the high-turbidity East China Sea is strongly influenced by the input of terrestrial material via the Changjiang River and the incursion of Kuroshio Current water. The nitracline shows four main structures (Structures 1–4, Fig. 4) in the East China Sea. Structure 1 mainly occurred in the coastal water and was primarily affected by the mixing of the Changjiang River diluted water and underlying water on the shelf. This nitracline had the opposite pattern of the halocline, with nitrate concentration decreasing with increased salinity. Structure 2 mainly showed a subsurface nitrate minimum in the halocline. Structure 3 mainly showed a nitrate maximum below the halocline; Structures 2 and 3 both occurred in the middle part of the shelf. Structure 4 mainly presented in the far-shore area and was associated with the incursion of the low-nutrient Kuroshio Current water, with the nitracline positively correlated with the halocline. The nitrate-poor condition in the surface water might be combined impact of biological uptake and low-nutrient water instruction.

4 Conclusions

We compared ISUS-measured nitrate concentrations and conventional bottle results across the East China Sea and Chuk-

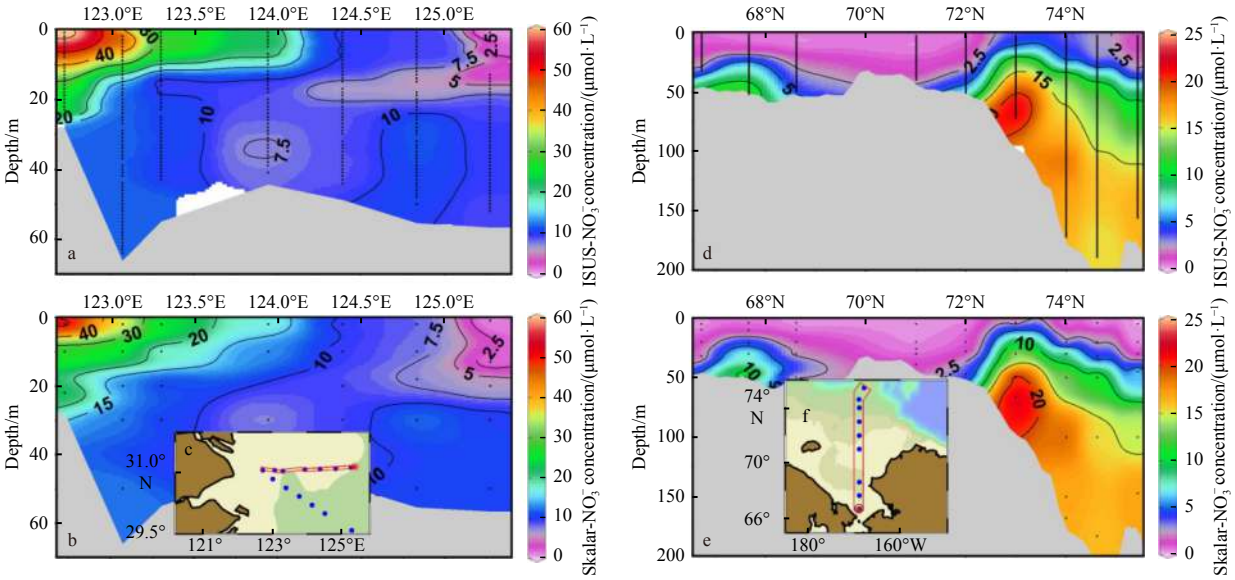

Fig. 3. Distributions of nitrate obtained by high-resolution measurements (ISUS-NO_3^-) and conventional techniques (Skalar-NO_3^-) on the East China Sea and Chukchi Sea. ISUS-NO_3^- (a) and Skalar-NO_3^- (b) data across the East China Sea, and location of the sampling transect (c). d–f demonstrate similar relationship with a–c, but for the Chukchi Sea shelf. Note that the data of ISUS-NO_3^- are the original values.

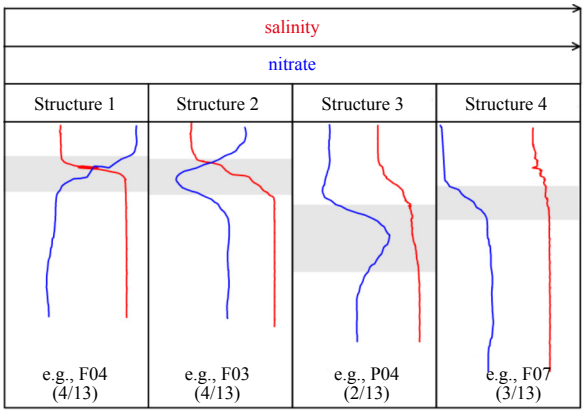

Fig. 4. Characteristics of the nitracline on the high-turbidity East China Sea, which is influenced by the Changjiang River. Red and blue lines represent salinity and nitrate concentration, respectively. The nitracline had four main structures (Structures 1–4). The figures in parentheses are the number of sampling sites where each structure was observed. Sites F04, F03, P04 and F07 refer to Fig. 1.

chi Sea, and found good agreement in low-turbidity waters. In the high-turbidity waters of the East China Sea (salinity<30), a correction factor of 1.19 was applied to the ISUS data in order to match the bottle measurements. Note that the correction factor of 1.19 may not necessarily be extrapolated to other seasons in the East China Sea or other high-turbidity shelves/regions, because interfering species (e.g., CDOM) vary with seasons and different waters.

The high-resolution nitrate data revealed subtle spatial variability (e.g., a subsurface nitrate minimum) that might not have been captured by the bottle results. The ISUS nitrate data show four main nitracline structures on the East China Sea. The results show that the ISUS optical nitrate sensor is capable of high-resolution, accurate measurements in both high- and low-turbidity waters. The high-resolution data are important for assessing nitrate budgets and nutrient dynamics on continental shelves.

Acknowledgements

We thank the crews of the icebreaker *Xuelong* and the R/V *Dongfanghong 2* during scientific survey.

References

Bauer J E, Cai Weijun, Raymond P A, et al. 2013. The changing carbon cycle of the coastal ocean. Nature, 504(7478): 61–70, doi: 10.1038/nature12857

Chen Fajin, Chen Jianfang, Jia Guodong, et al. 2013. Nitrate $\delta^{15}N$ and $\delta^{18}O$ evidence for active biological transformation in the Changjiang Estuary and the adjacent East China Sea. Acta Oceanologica Sinica, 32(4): 11–17, doi: 10.1007/s13131-013-0294-4

Chen Chen-Tung Arthur, Wang Shulun. 1999. Carbon, alkalinity and nutrient budgets on the East China Sea continental shelf. Journal of Geophysical Research: Oceans, 104(C9): 20675–20686, doi: 10.1029/1999JC900055

Chen Fajin, Zhou Xin, Lao Qibin, et al. 2019. Dual isotopic evidence for nitrate sources and active biological transformation in the northern South China Sea in summer. PLoS ONE, 14(1): e0209287, doi: 10.1371/journal.pone.0209287

Cloern J E. 2001. Our evolving conceptual model of the coastal eutrophication problem. Marine Ecology Progress Series, 210: 223–253, doi: 10.3354/meps210223

Finch M S, Hydes D J, Clayson C H, et al. 1998. A low power ultra violet spectrophotometer for measurement of nitrate in seawater: introduction, calibration and initial sea trials. Analytica Chimica Acta, 377(2–3): 167–177

Grasshoff K, Kremling K, Ehrhardt M. 2009. Methods of Seawater Analysis. New York: John Wiley & Sons

Guo Weidong, Stedmon C A, Han Yuchao, et al. 2007. The conservative and non-conservative behavior of chromophoric dissolved organic matter in Chinese estuarine waters. Marine Chemistry, 107(3): 357–366, doi: 10.1016/j.marchem.2007.03.006

Guo Weidong, Yang Liyang, Zhai Weidong, et al. 2014. Runoff-mediated seasonal oscillation in the dynamics of dissolved organic matter in different branches of a large bifurcated estuary—The Changjiang Estuary. Journal of Geophysical Research: Biogeosciences, 119(5): 776–793, doi: 10.1002/2013JG002540

Johnson K S. 2010. Simultaneous measurements of nitrate, oxygen, and carbon dioxide on oceanographic moorings: Observing the Redfield ratio in real time. Limnology and Oceanography, 55(2): 615–627, doi: 10.4319/lo.2010.55.2.0615

Johnson K S, Barry J P, Coletti L J, et al. 2011. Nitrate and oxygen flux across the sediment-water interface observed by eddy correlation measurements on the open continental shelf. Limnology and Oceanography: Methods, 9(11): 543–553, doi: 10.4319/lom.2011.9.543

Johnson K S, Coletti L J. 2002. In situ ultraviolet spectrophotometry for high resolution and long-term monitoring of nitrate, bromide and bisulfide in the ocean. Deep-Sea Research Part I: Oceanographic Research Papers, 49(7): 1291–1305, doi: 10.1016/S0967-0637(02)00020-1

Johnson K S, Coletti L J, Chavez F P. 2006. Diel nitrate cycles observed with *in situ* sensors predict monthly and annual new production. Deep-Sea Research Part I: Oceanographic Research Papers, 53(3): 561–573, doi: 10.1016/j.dsr.2005.12.004

Johnson K S, Coletti L J, Jannasch H W, et al. 2013. Long-term nitrate measurements in the ocean using the *in situ* ultraviolet spectrophotometer: sensor integration into the APEX profiling float. Journal of Atmospheric & Oceanic Technology, 30(8): 1854–1866

Johnson K S, Needoba J A. 2008. Mapping the spatial variability of plankton metabolism using nitrate and oxygen sensors on an autonomous underwater vehicle. Limnology and Oceanography, 53: 2237–2250, doi: 10.4319/lo.2008.53.5_part_2.2237

Johnson K S, Plant J N, Dunne J P, et al. 2017. Annual nitrate drawdown observed by SOCCOM profiling floats and the relationship to annual net community production. Journal of Geophysical Research: Oceans, 122(8): 6668–6683, doi: 10.1002/2017JC012839

Johnson K S, Riser S C, Karl D M. 2010. Nitrate supply from deep to near-surface waters of the North Pacific subtropical gyre. Nature, 465(7301): 1062–1065, doi: 10.1038/nature09170

Kaplunenko D D, Lobanov V B, Tishchenko P Y, et al. 2013. Nitrate *in situ* measurements in the northern Japan Sea. Deep-Sea Research Part II: Topical Studies in Oceanography, 86–87: 10–18

Khandelwal A, González-Pinzón R, Regier P, et al. 2020. Introducing the self-cleaning filtration for water quality sensors (SC-FLAWLeSS) system. Limnology and Oceanography: Methods, 18(9): 467–476, doi: 10.1002/lom3.10377

Li Yangjie, Jin Haiyan, Chen Jianfang, et al. 2021. Nitrogen removal through sediment denitrification in the Yangtze Estuary and its adjacent East China Sea: A nitrate limited process during summertime. Science of the Total Environment, 795: 148616, doi: 10.1016/j.scitotenv.2021.148616

Liu Sumei, Qi Xiaohong, Li Xiaona, et al. 2016. Nutrient dynamics from the Changjiang (Yangtze River) Estuary to the East China Sea. Journal of Marine Systems, 154: 15–27, doi: 10.1016/j.jmarsys.2015.05.010

Liu J P, Xu K H, Li A C, et al. 2007. Flux and fate of Yangtze River sediment delivered to the East China Sea. Geomorphology, 85(3–4): 208–224

MacIntyre G, Plache B, Lewis M R, et al. 2009. ISUS/SUNA nitrate measurements in networked ocean observing systems. In: OCEANS 2009. Biloxi, MS, USA: IEEE, 1–7

Mao Zhihua, Chen Jianyu, Pan Delu, et al. 2012. A regional remote sensing algorithm for total suspended matter in the East China Sea. Remote Sensing of Environment, 124: 819–831, doi: 10.1016/j.rse.2012.06.014

Meyer D, Prien R D, Rautmann L, et al. 2018. *In situ* determination of nitrate and hydrogen sulfide in the Baltic Sea using an ultraviolet spectrophotometer. Frontiers in Marine Science, 5: 431, doi: 10.3389/fmars.2018.00431

Pellerin B A, Bergamaschi B A, Gilliom R J, et al. 2014. Mississippi River nitrate loads from high frequency sensor measurements and regression-based load estimation. Environmental Science & Technology, 48(21): 12612–12619

Pidcock R, Srokosz M, Allen J, et al. 2010. A novel integration of an ultraviolet nitrate sensor on board a towed vehicle for mapping open-ocean submesoscale nitrate variability. Journal of Atmospheric & Oceanic Technology, 27(8): 1410–1416

Prien R D. 2007. The future of chemical *in situ* sensors. Marine Chemistry, 107(3): 422–432, doi: 10.1016/j.marchem.2007.01.014

Randelhoff A, Guthrie J D. 2016. Regional patterns in current and future export production in the central Arctic Ocean quantified from nitrate fluxes. Geophysical Research Letters, 43(16): 8600–8608, doi: 10.1002/2016GL070252

Rönnberg C, Bonsdorff E. 2004. Baltic Sea eutrophication: area-specific ecological consequences. Hydrobiologia, 514(1–3): 227–241

Sakamoto C M, Johnson K S, Coletti L J. 2009. Improved algorithm for the computation of nitrate concentrations in seawater using an *in situ* ultraviolet spectrophotometer. Limnology and Oceanography: Methods, 7(1): 132–143, doi: 10.4319/lom.2009.7.132

Sakamoto C M, Johnson K S, Coletti L J, et al. 2017. Pressure correction for the computation of nitrate concentrations in seawater using an *in situ* ultraviolet spectrophotometer. Limnology and Oceanography: Methods, 15(10): 897–902, doi: 10.1002/lom3.10209

Schlitzer R. 2018. Ocean Data View. http://odv.awi.de[2018-04-04/2019-12-03]

Wang Bin, Chen Jianfang, Jin Haiyan, et al. 2017. Diatom bloom-derived bottom water hypoxia off the Changjiang Estuary, with and without typhoon influence. Limnology and Oceanography, 62(4): 1552–1569, doi: 10.1002/lno.10517

Wang Baodong, Wang Xiulin, Zhan Run. 2003. Nutrient conditions in the Yellow Sea and the East China Sea. Estuarine, Coastal and Shelf Science, 58(1): 127–136

Wang Baodong, Wei Qinsheng, Chen Jianfang, et al. 2012. Annual cycle of hypoxia off the Changjiang (Yangtze River) Estuary. Marine Environmental Research, 77: 1–5, doi: 10.1016/j.marenvres.2011.12.007

Yan Weijin, Zhang Shen, Sun Pu, et al. 2003. How do nitrogen inputs to the Changjiang basin impact the Changjiang River nitrate: A temporal analysis for 1968–1997. Global Biogeochemical Cycles, 17(4): 1091, doi: 10.1029/2002GB002029

Zhai Weidong, Dai Minhan. 2009. On the seasonal variation of air-sea CO_2 fluxes in the outer Changjiang (Yangtze River) Estuary, East China Sea. Marine Chemistry, 117(1–4): 2–10

Zhang Jing, Liu Sumei, Ren Jingling, et al. 2007. Nutrient gradients from the eutrophic Changjiang (Yangtze River) Estuary to the oligotrophic Kuroshio waters and re-evaluation of budgets for the East China Sea Shelf. Progress in Oceanography, 74(4): 449–478, doi: 10.1016/j.pocean.2007.04.019

Zhou Feng, Xue Huijie, Huang Daji, et al. 2015. Cross-shelf exchange in the shelf of the East China Sea. Journal of Geophysical Research: Oceans, 120(3): 1545–1572, doi: 10.1002/2014JC010567

Zhuang Yanpei, Jin Haiyan, Cai Weijun, et al. 2021a. Freshening leads to a three-decade trend of declining nutrients in the western Arctic Ocean. Environmental Research Letters, 16(5): 054047, doi: 10.1088/1748-9326/abf58b

Zhuang Yanpei, Jin Haiyan, Chen Jianfang, et al. 2020. Phytoplankton community structure at subsurface chlorophyll maxima on the western Arctic shelf: patterns, causes, and ecological importance. Journal of Geophysical Research: Biogeosciences, 125(6): e2019JG005570, doi: 10.1029/2019JG0005570

Zhuang Yanpei, Jin Haiyan, Gu Fan, et al. 2017. Composition of algal pigments in surface freshen layer after ice melt in the central Arctic. Acta Oceanologica Sinica, 36(8): 122–130, doi: 10.1007/s13131-017-1024-0

Zhuang Yanpei, Jin Haiyan, Li Hongliang, et al. 2016. Pacific inflow control on phytoplankton community in the Eastern Chukchi Shelf during summer. Continental Shelf Research, 129: 23–32, doi: 10.1016/j.csr.2016.09.010

Zhuang Yanpei, Jin Haiyan, Zhang Yang, et al. 2021b. Incursion of Alaska Coastal Water as a mechanism promoting small phytoplankton in the western Arctic Ocean. Progress in Oceanography, 197: 102639, doi: 10.1016/j.pocean.2021.102639

Supplementary information:

Fig. S1. High-resolution nitrate measurements by the ISUS for evaluating the detailed structures of the nitracline along Transects P and F on the high-turbidity East China Sea.

Fig. S2. High-resolution nitrate measurements by the ISUS for evaluating the detailed structures of the nitracline along Transect R on the low-turbidity Chukchi Sea.

Table S1. Information about sampling stations and environmental variables in the East China Sea from a summer cruise of 2011.

Table S2. Information about sampling stations and environmental variables in the Chukchi Sea from a summer cruise of 2014.

The supplementary information is available online at https://doi.org/10.1007/s13131-022-2038-9 and http://www.aosocean.com/. The supplementary information is published as submitted, without typesetting or editing. The responsibility for scientific accuracy and content remains entirely with the authors.